

Momber, Ilan; Dallinger, David; Beer, Sebastian; Gomez, Tomás; Wietschel, Martin

## Working Paper

# Optimizing plug-in electric vehicle charging in interaction with a small office building

Working Paper Sustainability and Innovation, No. S9/2011

## Provided in Cooperation with:

Fraunhofer Institute for Systems and Innovation Research ISI

*Suggested Citation:* Momber, Ilan; Dallinger, David; Beer, Sebastian; Gomez, Tomás; Wietschel, Martin (2011) : Optimizing plug-in electric vehicle charging in interaction with a small office building, Working Paper Sustainability and Innovation, No. S9/2011, Fraunhofer-Institut für System- und Innovationsforschung ISI, Karlsruhe, <https://doi.org/10.24406/publica-fhg-295469>

This Version is available at:

<https://hdl.handle.net/10419/50780>

### Standard-Nutzungsbedingungen:

Die Dokumente auf EconStor dürfen zu eigenen wissenschaftlichen Zwecken und zum Privatgebrauch gespeichert und kopiert werden.

Sie dürfen die Dokumente nicht für öffentliche oder kommerzielle Zwecke vervielfältigen, öffentlich ausstellen, öffentlich zugänglich machen, vertreiben oder anderweitig nutzen.

Sofern die Verfasser die Dokumente unter Open-Content-Lizenzen (insbesondere CC-Lizenzen) zur Verfügung gestellt haben sollten, gelten abweichend von diesen Nutzungsbedingungen die in der dort genannten Lizenz gewährten Nutzungsrechte.

### Terms of use:

*Documents in EconStor may be saved and copied for your personal and scholarly purposes.*

*You are not to copy documents for public or commercial purposes, to exhibit the documents publicly, to make them publicly available on the internet, or to distribute or otherwise use the documents in public.*

*If the documents have been made available under an Open Content Licence (especially Creative Commons Licences), you may exercise further usage rights as specified in the indicated licence.*

Working Paper Sustainability and Innovation  
No. S 9/2011



**Ilan Momber**  
**David Dallinger**  
**Sebastian Beer**  
**Tomás Gomez**  
**Martin Wietschel**

Optimizing plug-in electric vehicle charging  
in interaction with a small office building

## **Abstract**

This paper considers the integration of plug-in electric vehicles (PEVs) in micro-grids. Extending a theoretical framework for mobile storage connection, the economic analysis here turns to the interactions of commuters and their driving behavior with office buildings.

An illustrative example for a real office building is reported. The chosen system includes solar thermal, photovoltaic, combined heat and power generation as well as an array of plug-in electric vehicles with a combined aggregated capacity of 864 kWh. With the benefit-sharing mechanism proposed here and idealized circumstances, estimated cost savings of 5% are possible.

Different pricing schemes were applied which include flat rates, demand charges, as well as hourly variable final customer tariffs and their effects on the operation of intermittent storage were revealed and examined in detail. Because the plug-in electric vehicle connection coincides with peak heat and electricity loads as well as solar radiation, it is possible to shift energy demand as desired in order to realize cost savings.

## **Key words**

Battery storage, building management systems, dispersed storage and generation, electric vehicles, load management, microgrid, optimization methods, power system economics, road vehicle electric propulsion

# Table of Contents

	Page
<b>1 Introduction.....</b>	<b>1</b>
<b>2 A Model For V2B Application.....</b>	<b>3</b>
<b>3 Illustrative Study.....</b>	<b>13</b>
<b>4 Price Discussion and Tariff Scenarios.....</b>	<b>21</b>
<b>5 Results.....</b>	<b>24</b>
<b>6 Conclusion.....</b>	<b>35</b>
<b>7 Acknowledgements.....</b>	<b>37</b>
<b>8 References.....</b>	<b>37</b>



## Figures

	Page
Figure 1:	Energy flows in a building microgrid .....3
Figure 2:	Energy flows in the model for PEV storage connection .....9
Figure 3:	<i>HMD<sub>h</sub></i> Fraunhofer ISI heat end use requirements on weekdays .....16
Figure 4:	<i>DMD<sub>h</sub></i> Fraunhofer ISI weekday electricity end-use requirements .....17
Figure 5:	<i>ISR<sub>h</sub></i> incident solar radiation by month in Karlsruhe .....18
Figure 6:	Composition of end-user electricity prices .....22
Figure 7:	Price curves for January by type days in Scenarios 1 – 4 .....24
Figure 8:	PEV Operation schedules on peak days for Scenarios 1 and 2 .....27
Figure 9:	Diurnal Microgrid Analysis for Peak Days in Scenario 1 .....28
Figure 10:	Resulting utility electricity purchases on peak days: Scenario 2 .....29
Figure 11:	Electricity balance: microgrid analysis December peak day: Scenario 2 .....30
Figure 12:	Electricity balance: microgrid analysis September peak day: Scenario 2 .....30
Figure 13:	Heat balance: microgrid analysis September peak day: Scenario 2 .....31
Figure 14:	Electricity balance: microgrid analysis May peak day: Scenario 3 .....32
Figure 15:	Electricity balance: microgrid analysis July peak day: Scenario 3 .....33
Figure 16:	Electricity balance: microgrid analysis May peak day: Scenario 4 .....34
Figure 17:	Electricity balance: microgrid analysis September peak day: Scenario 4 .....34

## Tables

	Page
Table 1: Input Parameters .....	6
Table 2: Decision variables .....	8
Table 3: Summary of input parameters .....	20
Table 4: High Level Numerical Summary - ISI Cost Minimization.....	26

# 1 Introduction

Alternative forms of mobility such as electric personal vehicles span a vast range of topics overlapping various disciplines. The success of this emerging technology, however, depends on end-user acceptance and market adoption, both of which presuppose economic viability. The feature of plug-in electric vehicles (PEVs) which is especially attractive to the energy industry as well as vehicle users is the capability to store energy. For the former, this is used in order to perform grid services, while for the latter this ultimately serves mobility needs (Kempton and Tomic 2005; KEMA Inc. and ISO/RTO Council 2010). General integration frameworks covering both technical operation and electricity markets have been proposed (Lopes, Soares, and Almeida 2011). However, depending on whether there is private or public access to charging points, the contractual relations among the interacting agents of the electric power industry can change. Classifying charging scenarios reveals certain implications for new legislation on reselling charging agents (Momber et al. 2011).

Furthermore, the underlying question remains: How can we measure the attractiveness of this new technology monetarily and put a value on electric vehicles for the different agents in the electric power system of the future? Research aims at finding the best points of access to the grid among charging alternatives. Where and how should electric vehicles be optimally employed for all the interested groups?

Business models need to be developed. These should define economic contracts between interacting participants and the resulting surplus distribution. Analyses of the dependence of these models on the electricity markets, ancillary services, utility tariffs, mobility patterns, connection behavior and billing contracts should be performed and thoroughly evaluated.

This study aims to quantify the value of vehicle storage both to the electricity grid and to the driver in a number of ways. Foremost, it endeavors to extend the application of electric vehicles and their storage characteristics to other fields that allow for economic deployment and efficient profitable use of batteries.

Public charging infrastructure remains a controversial topic as far as investment and ownership is concerned; different market models for the roll-out of public charging infrastructures are being discussed (EURELECTRIC 2010).

As the EU wants to facilitate end-user access to variable energy prices in order to incentivize efficient use, the objective of this paper is to develop a model that



simulates the charging response to equivalent price volatility by applying a scenario with more and more fluctuation of prices. The effects of intermittent renewable generation from wind and solar power are visible today on the European electricity exchange market and even result in hours with negative prices.

Regardless of the ownership structure, the application of lithium-ion batteries in electric vehicles heavily influences the capital costs associated with degradation. Similar to any other investment in technologies, the shorter the life of the battery is, the higher are the discounted monetary burdens per time period. Factors such as the capacity, charging rate, cost, cycle life and calendar life are all critical in making batteries commercially and economically viable for EVs. Many of these factors are still largely unknown and have never been tested under real-life conditions and actual time frames. Yet they all have a considerable impact on the value proposition. In order to reach a clear conclusion, the spectrum of battery degradation rates due to both cycle life and calendar life in various climates and operating SOC is needed (Pesaran, Smith, and Markel 2009).

Knowing that people's actual behavior contains a degree of complexity that is hard to capture in modeling, this paper relies on a simplistic approach to obtain a best estimate of battery degradation due to its operation in interaction with buildings. This best estimate is considered to be the energy throughput processed by the battery and cycled in relation to its capacity (Peterson, Apt, and Whitacre 2010).

Moreover, based on earlier proposals for business models, it properly integrates electric vehicles on a small scale, so-called microgrids, for instance office buildings with sophisticated on-site management systems. It seeks to highlight load management possibilities in an electricity grid with smart control of devices and generators.

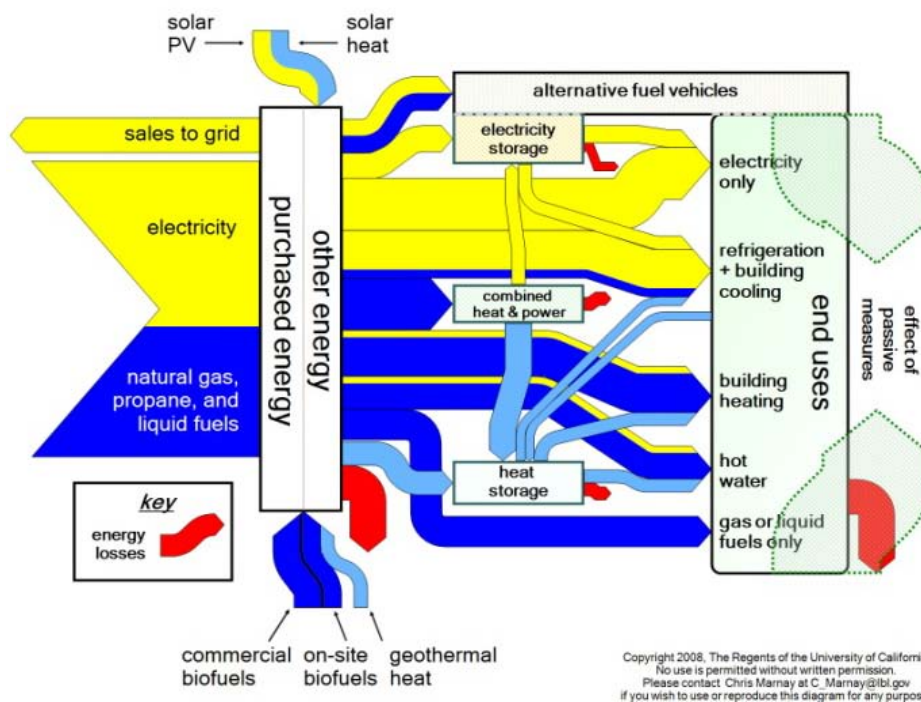
Concerning the structure of this document: section II. establishes the theoretical foundations for extending the existing model including a description of the input parameters, decision variables, objective functions and an electricity flow schematic. Section III. applies the theoretical model to plug-in electric vehicle interactions with office buildings for a particular case. Section IV. describes the four fundamental pricing scheme scenarios that form the core of the analysis. Section V. presents the results concerning electricity and heat balancing operation schedules and compares them to each other. Finally, section VI draws conclusions and highlights the value of this study.

## 2 A Model For V2B Application

The optimization of plug-in electric vehicle storage is embedded within the Distributed Energy Resources - Customer Adoption Model (DER-CAM).

DER-CAM solves a commercial building's microgrid investment and operation optimization problem given its end-use energy loads, energy tariff structures and fuel prices, and an arbitrary list of equipment investment options. The Sankey diagram in Fig. 1 shows energy flows in a building scale microgrid/smartgrid and illustrates how DER-CAM operates. DER-CAM solves the system analytically by representing it as a mixed integer linear program written on the GAMS® platform. Regulatory, engineering, and investment constraints are all considered. Energy costs are calculated using a detailed representation of utility tariff structures and fuel prices, operating and maintenance (O&M) expenditures, as well as any amortized DER investment outlays.

Figure 1: Energy flows in a building microgrid



Optimal combinations of equipment involving PV, thermal generation with heat recovery, thermal heat collection, heat-activated cooling, and both thermal and electrical storage can be identified in a way intractable by simple searching. DER-CAM can report a cost, carbon footprint, or combination minimizing equipment choice and (typically hourly) optimal operating schedule for the microgrid/smartgrid, including CHP and renewable sources. The economics of

storage are particularly complex, both because they require optimization across multiple time steps and because of the strong influence of tariff structures. This research focuses on the upper right part of Fig. 1, where alternative fuel vehicles appears.

More information on DER-CAM can be found at C. Marnay et al. 2008, Siddiqui et al. 2005. Similar DER-CAM work on electric vehicles for buildings can be found at Stadler et al. 2011.

In the following, an excerpt of the DER-CAM mixed integer linear optimization problem (MILP) is presented. It is not exhaustive as it only contains the relevant information concerning PEV and building interactions; it omits the description of all other constraints for generation technologies and reduces the complexity of regulated tariffs. It is formulated for a period of one year and only includes the information concerning the building's contract and payments to PEVs, focusing on the energy balance of the intermittent mobile storage devices. The links to the platform model are the deterministic electricity demand and energy supply prices in particular. The latter is of special importance, because this formulation simplifies to an hourly value, even though demand charges and other more complex tariff components could be enclosed in this price.

## A. Input Parameters

The input parameters in Table 1 include information about the investment conditions, battery degradation, storage technology costs, decay behavior and efficiencies, operational restrictions as well as mobility assumptions about the PEV connection.

### 1) Building input

The electricity demand for each hour  $DMD_h$ , the heat demand  $HMD_h$  and the hourly electricity price  $P_{supply}$  taken from the contract with the utility supply company are the main parameters that define the building input in interaction with PEVs.  $P_{supply}$  is called "resolved" as it stands for more than just an hourly value.

### 2) Building to PEV contracts

Assuming that the PEVs offer a monetary benefit to the building, it can invest in contracting the vehicles. The interest rate  $I$  stands for the conditions for alternative investments on the capital markets for opportunity investment options. The duration of the contract  $T$  stands for the length of the agreement to interact. The

initial outlay is divided into a fixed part  $F$  that is paid regardless of the amount of storage that the building invests in, and a variable part,  $V$ , that is multiplied by the storage capacity.  $P_{EX,EV}$  is the hourly price used to value the energy exchange between the fleet of PEVs and the building. The price of alternative PEV charging is designated the offsite access opportunity price.

### 3) **Battery degradation**

The third set of input parameters refers to the capacity degradation of the batteries. In the model they are continuously scalable, i.e. their size can be chosen freely and have any positive real number. These parameters contain a coefficient  $D$  and a long-term production cost  $CP$  for replacing the batteries.

### 4) **PEV mobility behaviour**

$SOC_{in}$  stands for the state of charge of the aggregated PEV batteries at the hour ('in') of connecting the cars. Correspondingly,  $SOC_{out}$  indicates the state of charge when the aggregated PEV batteries are disconnected in order to provide mobility services. Note that this implies the PEV owner needs to know what his travel plans are in order to convey this information to the building.  $BCT_h$  summarizes this information and indicates when the PEV batteries are controlled by the EMS and available for optimizing building purposes. This is done in the form of a binary array.

### 5) **Operational battery input**

and denote the maximum relative charge and discharge rate amenable to the system as a fraction of the rated capacity that can be processed in one hour. In the literature these are often abbreviated C-rates and for these types of batteries usually not constrained by chemistry but by the capacity limit of the PEV power connection with the building. The efficiency parameters for charging and discharging emphasize the fact that certain losses arise when storing electrical charge. The decay factor takes all the charge losses over time into consideration, i.e. from one hour to the next.

Table 1: Input Parameters

	Description	Symbol	Unit
Building input	Electricity demand by the building	$DMD_h$	kWh
	Heat demand by the building	$HMD_h$	kWh
	Resolved hourly electricity price	$P_{supply,h}$	€/kWh
Investment contracts	Interest rate	$I$	%
	Duration of contract	$T$	a
	Fixed cost of scalable investment	$F$	\$
	Variable cost of scalable investment	$V$	€/kWh
	Hourly price for net energy exchange	$P_{EX,EV}$	€/kWh
	Offsite access opportunity price	$P_{offsite\ Access}$	€/kWh
Battery	Cost of production for Li-ion battery	$CP$	€/kWh
	Capacity degradation coefficient	$D$	%
Mobility	SOC of PEV batteries at disconnection	$SOC_{in}$	%
	SOC of PEV batteries at connection	$SOC_{out}$	%
	Connection array	$BCT_h$	
Operational battery input	Maximum relative charge rate		% * h <sup>-1</sup>
	Charge efficiency		%
	Maximum relative discharge rate		% * h <sup>-1</sup>
	Discharge efficiency		%
	Decay factor		%
	Minimum SOC	—	%
	Maximum SOC		%

## B. Decision variables

The decision variables in Table 2 consist of the investment level planning, operation schedule and the energy exchange schedule at the building interface.

### 1) Investment level planning

On the one hand, the planning level can freely scale the size of the storage capacity needed. The variable  $c$  stands for the aggregated size of the vehicle fleet in kWh electricity storage.

## 2) **Operation schedule**

On the other hand, the operation program sets the optimal SOC for each hour  $soc_h$ , which results in the operation schedule that is most profitable for the building. In an attempt to explain the rest of the functionality in simple terms, it could be said that everything else derives from this. In order to attain these states of charge, the battery must be connected via energy inputs  $fi_h$  and  $i_h$  as well as energy outputs  $o_h$  and  $fo_h$  respectively.

## 3) **Building interface**

Once the investment level and the operational schedule have been determined, the consumption of the batteries  $cod_h$  as well as the generation  $pvd_h$  are deduced and the resulting load curve of the building  $pud_h$  is determined. If no other generation technology is adopted, as assumed in this presentation for the sake of simplification and understandability, the resulting load is purchased from the supply network.  $pvd_h$  stands for the electricity production by the photovoltaic arrays and  $pud_h$  is the generation of electricity from distributed CHP units. Finally,  $h_{d,h}$  depicts the heat demand met by natural gas purchases for boilers,  $h_{c,h}$  the heat collection from solar thermal units, and  $h_{g,h}$  is the generation of heat from distributed CHP units.

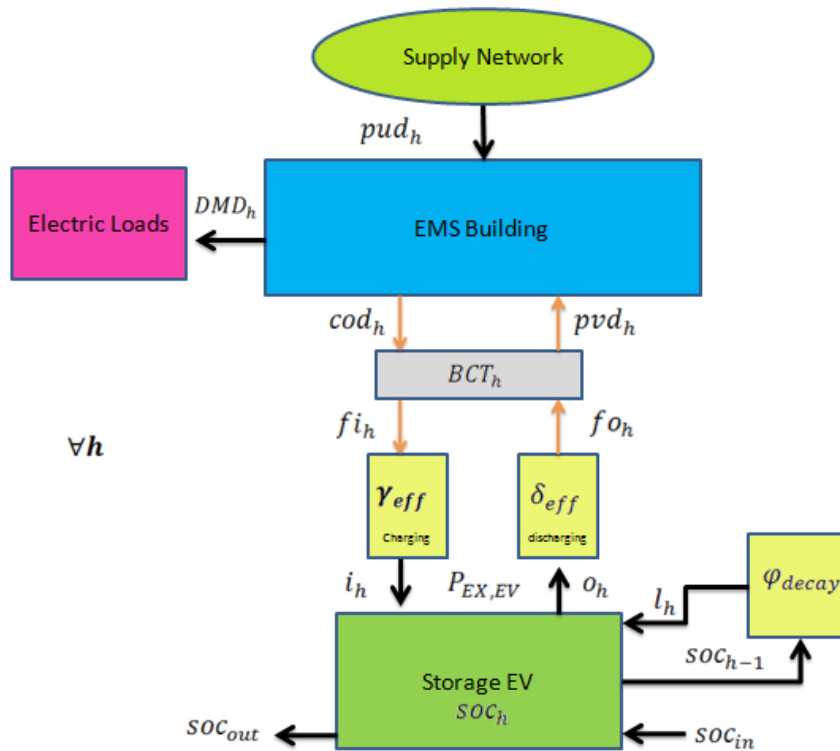
Table 2: Decision variables

	Description	Symbol	Unit
Operation schedule	Aggregated capacity of connected PEVs	$c$	kWh
	State of charge of PEV batteries	$soc_h$	kWh
	Energy output processed	$o_h$	kWh
	Efficient energy output processed	$fo_h$	kWh
	Energy input processed	$fi_h$	kWh
	Efficient energy input processed	$i_h$	kWh
	Energy losses due to battery decay	$l_h$	kWh
Building interface	Net energy flow batteries to EMS	$pvd_h$	kWh
	Net energy flow EMS to batteries	$cod_h$	kWh
	Electricity production of PV	$epv_h$	kWh
	Electricity production of CHP units	$edg_h$	kWh
	Heat provided by natural gas fired boilers	$hpd_h$	kWh
	Heat collected from solar thermal units	$hst_h$	kWh
	Heat produced from CPH units	$hdg_h$	kWh
	Resulting load curve	$pud_h$	kWh

### C) Electricity flow model

Figure 1 is provided to clarify the modeling of the energy flows in the PEV module. Each generation or storage technology is under the control of the energy management system (EMS). This is in charge of supplying the end use energy requirements  $DMD_h$  for the electricity loads. For each hour, it has the option to either procure energy from the supply network  $pud_h$  of the distribution grid, or use the PEV battery system  $pvd_h$ . The intermittent character of the PEVs and mobility behavior are marked by the binary connection table  $BCT_h$ . The modules which take efficiency losses for charging and discharging into account are denoted by transforming  $fi_h$  into  $i_h$  and changing  $o_h$ , into  $fo_h$ . Storage losses due to charge decay over time are captured by depending on the state of charge of the preceding hour. Figure 1 shows these electricity interactions in a flow diagram.

Figure 2: Energy flows in the model for PEV storage connection



**D) Algebraic formulation of the EMS optimization**

The optimization is integrated in the objective function, equations (1) – (4), of the EMS for the building, as shown in the algebra below. The building’s perspective is taken and the goal is to minimize the building’s electricity costs over the entire year subject to a set of operational constraints, see equations(7) –.(17)

**1) Objective function:**

$$\min_{\forall h} \sum_{h=1}^{8760} C_{elec} \cdot P_{EX,EV} \quad (1)$$

$$\min_{\forall h} \sum_{h=1}^{8760} C_{elec} \cdot P_{EX,EV} \quad (2)$$

$$\min_{\forall h} \sum_{h=1}^{8760} C_{elec} \cdot P_{EX,EV} \quad (3)$$



(4)

In the objective function the first term represents the initial contract investment, interpretable as a connection fee from the building to the PEV or a contribution to the purchase cost of the storage in order to compensate for the release of control to the building. The annuity factor distributes the initial outlay of the investment costs over the indicated periods and annualizes the expenses as calculatory costs.

(5)

The cost of investment can be divided into a fixed intercept part, e.g. for infrastructure, and a variable capacity, measured as the available storage capacity of the connected electric vehicle fleet. This modeling is convenient as it is directly comparable with the widely discussed costs for producing batteries (per kWh) as long as lifetime assumptions are consistent.

(6)

The second term stands for the degradation costs incurred due to the operation of the vehicles. If these are controlled by the EMS and serve the building's purposes, the compensation of battery degradation is a cost to the building.

Therefore the costs of degradation are split as follows, cf. equation (2): the monetary replacement cost is multiplied by the capacity degradation. According to the usage coefficient, i.e. all energy – charging and discharging – processed over initial capacity, the capacity degradation coefficient and the maximum amount of degradable capacity, i.e. 20 %<sup>1</sup>. This share of total initial capacity is then valued with the replacement cost of . In equation (2), the capacities would cancel each other out, but for clarity they are left as they are. The same is true for the denominator of the first term, where the trivial calculation would be (Peterson, Whitacre, and Apt 2010).

<sup>1</sup> USABC requirements for manufacturers' guarantee. Consequently, each percent of total name plate capacity equals 5 % in value degradation, assuming that there is no salvage value at 80 % name plate capacity.

Equation (3) bills the net energy exchange with PEVs, in this notation net output  $P_{net}$ , according to the agreed energy exchange price,  $P_{net}$ . Finally, the last equation accounts for the net energy procured from the supply network at the applicable tariff  $P_{net}$ .

## 2) **Constraints**

In equation (7) the SOC is defined and constrained: The SOC at any period of time is determined by the SOC from the preceding period plus the net input into the storage system in this period. This net hourly input is determined via the difference in input and output as well as the storage losses. Additionally, the state of charge can never exceed the maximum capacity. For given battery types, operational conditions and desired life, equation (8) ensures that the state of charge is kept within the boundaries for “healthy” operation. Also, in the form of a sandwich criterion, certain states of charge can be forced to be met at certain hours. The SOC input matrices, for instance, take care of non-availability during times of disconnection, forcing the storage system to meet the state of charge 0.

Equation (9) makes sure that energy output flows are kept within reasonable boundaries by charge rate constraints. The maximum charge rates depend on the storage capacity of the battery unit and the connection infrastructure. Analogously to the energy output flows, maximum charge rates regulate energy input with equation (10). A simple decay constraint takes into account that energy losses over time depend on the state of charge during the prior period, as equation (11) describes. Shown in equation (12), discharging efficiencies affect the amount of energy that is available to the energy management system of the building. These efficiencies are modeled as constants proportional to the output from the battery. Equation (13) for charging is in analogy to the discharging efficiencies. Some fraction of the energy provided by the building’s energy management system is lost and the input into the storage system is diminished.

The availability of the storage to the energy management system and to balance energy is limited to the times at which there is no connection or disconnection activity whatsoever. In consequence, energy amounts in the form of stored electricity leaving or entering the system, crossing system boundaries through connection or disconnection are neglected for the billing process. See equation (14) which expresses that the energy provided to the building is diminished by the amount brought in through connection. The energy the battery consumes is likewise diminished by the amount extracted through disconnection, see equation (15). Equation (16) describes the electricity balance for the building at each

period of time. The amount purchased from the energy supply network is equal to the exogenous demand plus the amount of consumption from battery charging minus the amount from discharging the battery and onsite production from photovoltaic and distributed generation (DG). Finally, the last equation refers to the heat demand that needs to be balanced: The net heat demand met by purchasing natural gas for the boilers needs to equal the given end use demand minus the heat collected from solar thermal units and the heat generated by the distributed CHP units.

(7)

—

(8)

(9)

(10)

(11)

(12)

(13)

(14)

(15)

(16)

(17)

In order to balance the benefits between the building and the PEV fleet, the following constraint for utilizing the batteries is introduced so that the owners at least break even. It describes the payment received by the owners of the PEV fleet. The annualized connection fee is paid at the beginning of a year and is expressed per unit of storage capacity. The second term regards the payment from the net energy exchange, which can be either a net charge or a net discharge. The left side of equation (18) depicts the main source of benefit for the EV owner. If the offsite access opportunity price is less than the exchange price discharging yields positive utility, whereas charging would be negative. Or it could be the other way around that <

, meaning that discharging would lead to negative utility for EV owners. This benefit should be at least equal to zero over the entire duration of the contract.

(18)

\_\_\_\_\_

\_\_\_\_\_

(19)

Having described the storage valuation model in detail on a conceptual and formal, mathematical level, the paper now looks at its application in the following case studies.

### **3 Illustrative Study**

Having evaluated the developed program based on a San Francisco Office building (Momber et al. 2010), a second case is introduced by applying the model to a Fraunhofer institute's office building. There are several reasons for doing so. Unlike the Californian example, electricity tariffs differ in Germany, i.e. there are flat energy rates as well as yearly demand charges, and end-user prices, i.e. special CHP and PV feed-in tariffs. Additionally, the European Union wants to facilitate end-user access to variable energy prices (EnWG 2005). The intention is to test the model's reaction to such price volatility by applying an end-user tariff with hourly tariffs pegged to the European energy exchange wholesale market. Finally, the specific mobility behavior of staff in the examined office building was derived from a survey conducted among the staff.

## **A. Relevant input**

### **1) *Mobility behavior***

To design the application case as realistically as possible and to provide an approach independent of high level data such as the *National Household Travel Survey*, *Mobility in Germany* or *Mobility Panel Germany*, a survey was conducted among the workers in the building under analysis to collect information about their driving behavior and commuter habits.

#### *a) Arrival and Departure Times*

The average arrival time is 8:40 a.m. for all weekdays and all staff taking part in this survey. The average departure time is 17:15 p.m. As a result the rational analyst would be inclined to choose the hours 8 h and 17 as suitable connection times for the hourly model.

#### *b) Average kilometers traveled and resulting states of charge*

Having found suitable connection times, the input parameters require the corresponding energy levels of the batteries relative to their total capacity.

The weighted average distance for all commuters, i.e. all participants of the survey, amounted to 5.0 km urban and 13.06 km rural driving for each trip to and from work, adding up to a total of 18.1 km one way and 36.2 km per day. Assuming there is seasonal variation, this value is varied by +10 % for summer and -10 % for winter. In analogy to the test case, this will serve as the basis for the SOC calculations (Momber et al. 2010).

However diverse the composition of the PEV fleet with different battery sizes might be, all vehicles are considered to have an average energy demand in charge depleting mode of 0.145 kWh/km (Peterson, Whitacre, and Apt 2010; Aksen, Burke, and Kurani 2008).

#### *c) Fleet size*

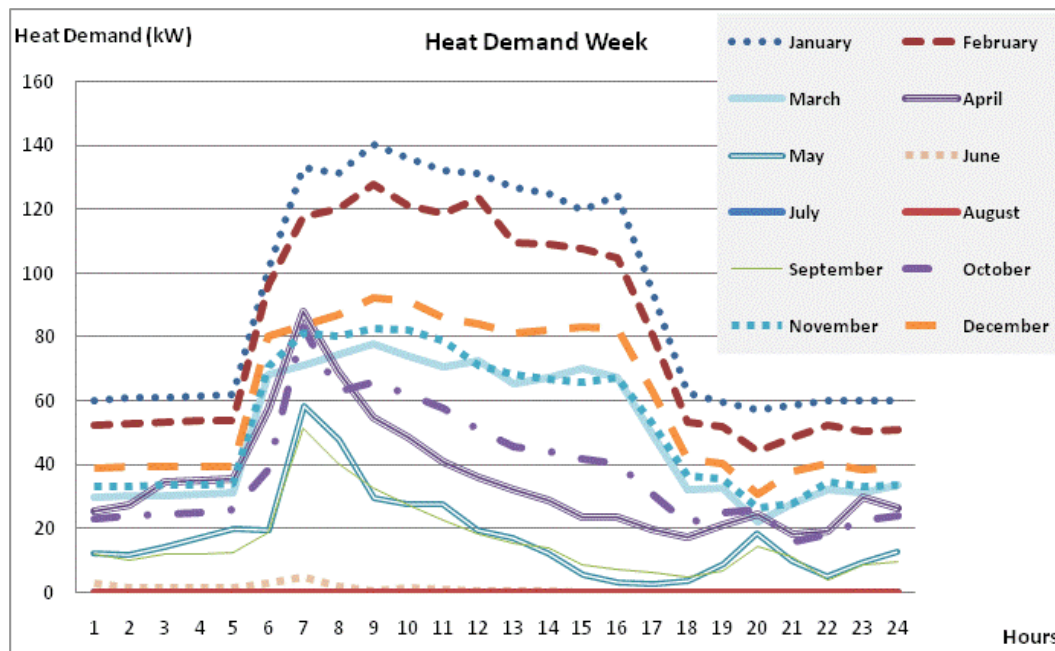
Promises to improve their commuting behavior are widespread among the office building's staff. Of the group in favor of innovative mobility concepts, the majority (39 %) perceives advantages in the use of a purely electric compact car with approximately 24 kWh, whereas 26 % regard a hybrid model with 16 kWh as their best choice, and 20 % prefer a regular sized car, here a BEV with 30 kWh. Merely 11 % consider a bicycle with supportive (1 kWh) electric propulsion and

4% are in favor of an electrified scooter with approximately 6 kWh. To come up with a potential storage quantity provided by this body of electric vehicle owners and users, the number of people within each group is weighted with the corresponding battery size of the vehicle class. The storage quantity of all vehicles would thus amount to 864 kWh which is a fixed parameter for the optimization in this case analysis.

## **2) *The office building's heat demand***

The heating system of the Fraunhofer ISI building was last renewed in 1996. It comprises two natural gas fired CHP units with 5.5 kW electric capacity and 12.5 kW heat recovery as well as two natural gas fired boilers with 90 kW and 210 kW peak capacities, respectively. They do not specifically have the function to instantly meet unusual heat demand but their production is variably scalable. The gas boilers were installed prior to the last modernization. Based on the technical specifications, the system's total efficiency should be relatively high, but no real data could be collected to substantiate this. However the information about the operation schedule of the units was sufficient to derive a significantly confident heat demand curve for the Fraunhofer office building. The 8760 operating hours of year 2009 were then aggregated to type day profiles for weekdays, weekends and peak, of which the weekday profile is shown in Figure 2.

Figure 3:  $HMD_h$  Fraunhofer ISI heat end use requirements on week-days



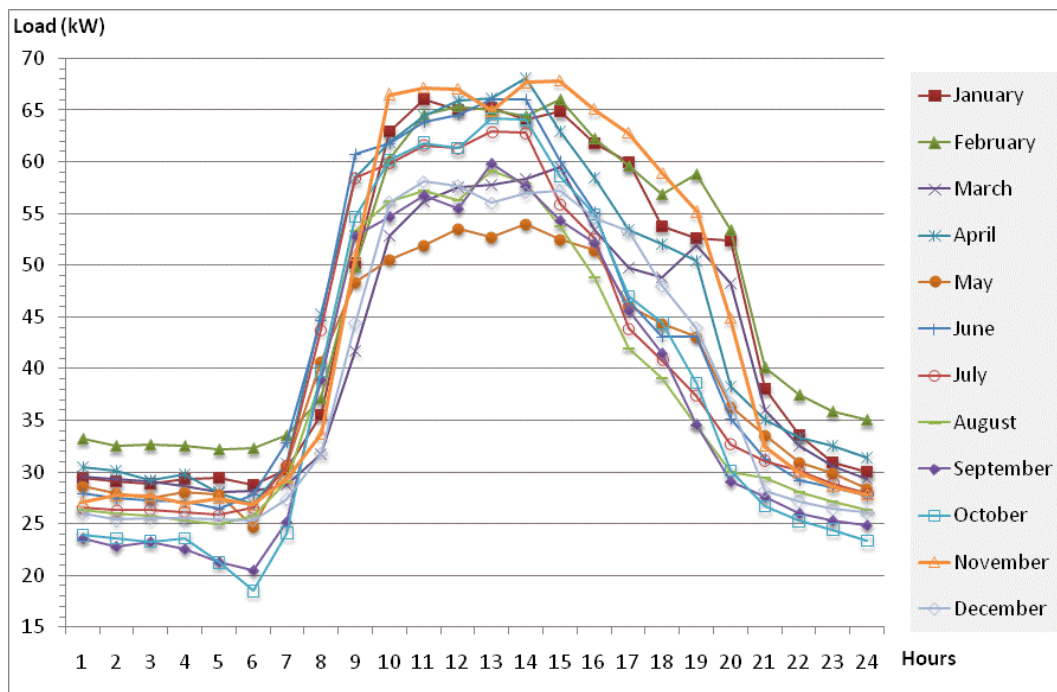
Evidently, during the off-peak hours from 18 h to 6 h, the system runs at a notably lower demand level. During morning hours demand is usually at its maximum to meet the building's imminent heat storage. Demand then gradually decreases over the day. Seasonal differences can be perceived; winter months tend to have a higher demand, clearly led by January and February, which must have been comparatively cold. November, December and March rank in a milder zone with 75 to 90 kW peaks. Summer months follow with lower heating activity. June, July and August, when the weather in Karlsruhe is fairly hot, present zero to almost zero demand. This heating system is exclusively designed for space heating and does not include water heating demand. The hot water in all sanitary units is provided by locally applied, small-scale electrical boilers as the lack of full load hours and a water heating infrastructure render ICEs unprofitable for these purposes.

### 3) *The office building's electricity demand*

For 2008, the time series data for electricity purchases was recorded by the utility company. The total end-use requirement, however, is divided up into own production by CHP units and procurement from the electricity supplier. The resulting diurnal electricity demand profile on weekdays is shown in Figure 4. It can be deduced that electricity consumption follows clear patterns throughout

the year. Electricity consumption strictly correlates with business activity in the building. The demand increases sharply in the morning, is at its maximum in the middle of the day and gradually decreases in the afternoon. There is a high base load of 25 to 35 kW caused by the data center and computer server facilities, while the peaks from regular business activity range from 50 to 65 kW on average weekdays.

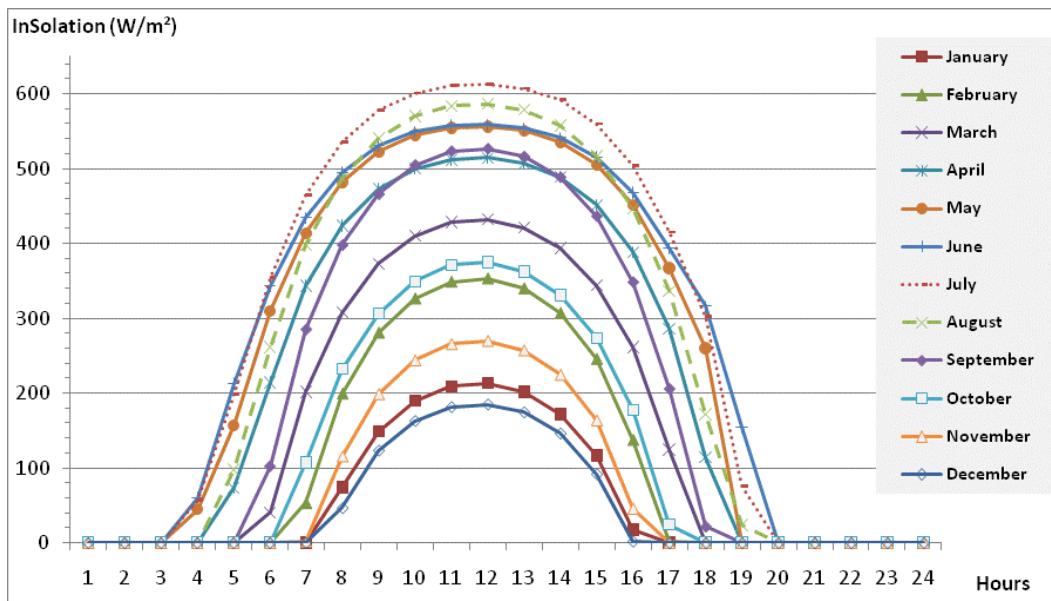
Figure 4:  $DMD_h$  Fraunhofer ISI weekday electricity end-use requirements



#### 4) Solar radiation

The model's input for incident solar radiation at the specific location of the Fraunhofer ISI office building in Karlsruhe is presented in Figure 4. It indicates the global solar irradiance for a south facing surface at 35° inclination and 0° azimuth with the coordinates 49° 2' 0" N, 8° 26' 0" E (Photovoltaic Geographical Information System (PVGIS) 2009).



Figure 5:  $ISR_h$  incident solar radiation by month in Karlsruhe

The values were averaged for diurnal schedules in an hourly resolution and for each month. The values follow a logical pattern with the highest and longest energy streams in summer, namely the month of August, and the lowest and shortest streams during winter, namely December. The energy intensity per area is directly converted to PV output by multiplying the insolation with the average PV efficiency of 13 %.

### 5) Other model settings

Table 3 presents a summary of all the parameter values. A 230 V, 16 A circuit infrastructure determines the energy exchange constraints at 3.68 kW exchanged. The charging rates therefore are restricted to  $12.267 \% h^{-1} = 3.68 \text{ kWh} \cdot h^{-1} / 30 \text{ kWh}$ . The real interest rate  $i$  for annuity calculations is 6%. Investment in charging infrastructure is assumed to be independent of connected battery capacity with a €5 connection payment  $F$ , while the duration of the contract is assumed to be one year, ( $T=1$ ). All payments are settled annually.

By averaging the crucial determinants, such as production volume, chemistry type, type of vehicle and battery pack size, the industry-wide production cost ( $CP$ ) for lithium-ion batteries is assumed to be around €200 per kWh in the long term (Momber et al. 2010).

The residential tariff under which electricity is purchased to charge the PEVs at home,  $P_{\text{offsite access}}$ , is assumed to amount to 23.6 €/kWh and remains constant

for all scenarios. This is the average residential rate for a household with an annual consumption of 3500 kWh in 2009, including wholesale prices with variable generation costs for fuels, transport and CO<sub>2</sub>, sales taxes of 19 %, as well as net access fees, concession levies, apportionments from the German Renewable Energies Act (EEG) and the German Combined Heat and Power Act (KWKG) (Dürr 2010). This price is also chosen for billing the metered net energy exchange between the PEVs and the building's EMS,  $P_{EX,EV}$ . This means that any energy exchange should be utility and benefit neutral for the driver of the electric vehicle. The owner and driver of the vehicle remain indifferent towards the resulting SOC when disconnecting as long as this remains within the specified boundaries. The main assumption here is that the connection payment compensates the PEV owner for giving up control as long as battery degradation is compensated.

## 6) *DER settings*

Apart from the PEV interface, the following assumptions are made. Depending on the time of use (TOU), the net price under the current gas tariff is 0.055 €/kWh for on-hours and 0.48 €/kWh for off-hours. To obtain an end user price for future scenarios, 0.06 €/kWh was assumed to be the flat gross price including sales taxes (Verbund Kommunalen Unternehmen 2006).

In this analysis, the main goal is to replicate the existing real time structure of the energy system at the Fraunhofer ISI office building and to derive the operation schedules for the PEV storage, and not to point out alternative investments to decrease costs or to increase the building's energy performance and efficiency. It was not intended to come up with subsidy price thresholds to indicate policy ways of facilitating certain technologies. Therefore the following information about continuous and discrete technology options was set as fixed input in the solution:

Two CHP units, Dachs internal combustion engines with heat exchangers by Senertec with 12.5 kW<sub>th</sub> – 5.5 kW<sub>el</sub>, capital costs of 3617.60 €/kW<sub>el</sub> depreciated over a lifetime of 20 years, 60.20 € fixed operation and maintenance cost per kW<sub>el</sub>/a, variable operation and maintenance cost of 0.037 €/kWh produced, 27 % electric fuel efficiency, 61 % thermal fuel efficiency (88 % combined), and therefore a heat to power ratio of 2.27.

The other distributed generator, Buderus ICE for heating are only considered indirectly. The model is not able to simulate the capital cost of central heating boilers. This does not pose any major difficulty here as the lifetime of these facilities can be assumed to have passed and all value has been depreciated.

Hence, operational costs merely occur in the form of natural gas purchases which are valued at their price. Solar thermal heat collectors with 20 kWp capacity, 1400 € fixed and 700 €/kWp variable investment costs, 15 years lifetime and 0.70 €/kWh maintenance are entered into the solution in order to have a higher number of heat sources. Today's photovoltaic arrays of 5 kWp were scaled up to 20 kWp with capital costs based on today's annualized 5000 € fixed and 3000 €/kWp variable investment costs, 20 years lifetime and 0.25 €/kWh maintenance cost (Rutschmann and Siemer 2009). Table 3 provides a summary of the input parameters described above for the Fraunhofer ISI building.

Table 3: Summary of input parameters

Description	Symbol	Value	Unit
Heat demand of the building	$HMD_h$	<b>Fig. 2</b>	kWh
Electricity demand of the building	$DMD_h$	<b>Fig. 3</b>	kWh
Incident solar radiation	$ISR_h$	<b>Fig. 4</b>	kWh
Resolved hourly electricity price	$P_{supply}$	<b>Fig. 5/6</b>	€/kWh
Interest rate	$I$	<b>6</b>	%
Duration of contract	$T$	<b>1</b>	a
Connection payment	$F$	<b>5</b>	€
Hourly net energy exchange price	$P_{EX,EV}$	<b>0.236</b>	€/kWh
Offsite access opportunity price	$P_{offsite}$	<b>0.236</b>	€/kWh
Production cost for Li-ion batteries	$CP$	<b>200</b>	€/kWh
Capacity degradation coefficient	$D$	<b>0.0027</b>	%
SOC batteries at disconnection	$SOC_{in}$	<b>71.97/75.25</b>	%
SOC batteries at connection	$SOC_{out}$	<b>38.03/34.75</b>	%
Connection array	$BCT_h$	<b>8h / 17h</b>	
Maximum relative charge rate		<b>12.267</b>	% h <sup>-1</sup>
Charge efficiency		<b>95.4</b>	%
Maximum relative discharge rate		<b>12.267</b>	% h <sup>-1</sup>
Discharge efficiency		<b>95.4</b>	%
Decay factor		<b>0.1</b>	%
Minimum SOC	—	<b>20</b>	%
Maximum SOC		<b>90</b>	%

## 4 Price Discussion and Tariff Scenarios

As the EU wants to facilitate end-user access to variable energy prices (Beyer, Heinemann, and Tusch 2009), the objective of this case study is to test the model's response to equivalent price volatility by applying different scenarios with increasing hourly fluctuation of prices. For this case study, the following four scenarios of electricity prices were chosen:

1. Today's actual electricity procurement tariff with the utility company Stadtwerke Karlsruhe in place.
2. An assumed regulated electricity procurement tariff with monthly demand charges similar to the Californian conditions of the test case (Momber et al. 2010).
3. Hourly varying prices pegged to historical price curves from the European Energy Exchange market data 2009.
4. Hourly varying prices pegged to simulations of the European Energy Exchange for the year 2030 considering climate change and e-mobility deployment.

### 1) **Scenario 1: Base case – today's electricity tariff**

The real electricity supply tariff currently applied to the discussed office building is rather simple in its structure. The energy rates are flat and set at  $P_{supply} = 15.66 \text{ €ct/kWh}$  regardless of the TOU. This price is the gross cost including sales taxes, EEG and KWKG payments. There is a demand charge that prices the maximum load over the entire year, starting with the contract date. Compared to the US tariff evaluated in the test case, this would not be called a monthly but a yearly demand rate and amounts to  $47.86 \text{ €/kW}$  peak demand.

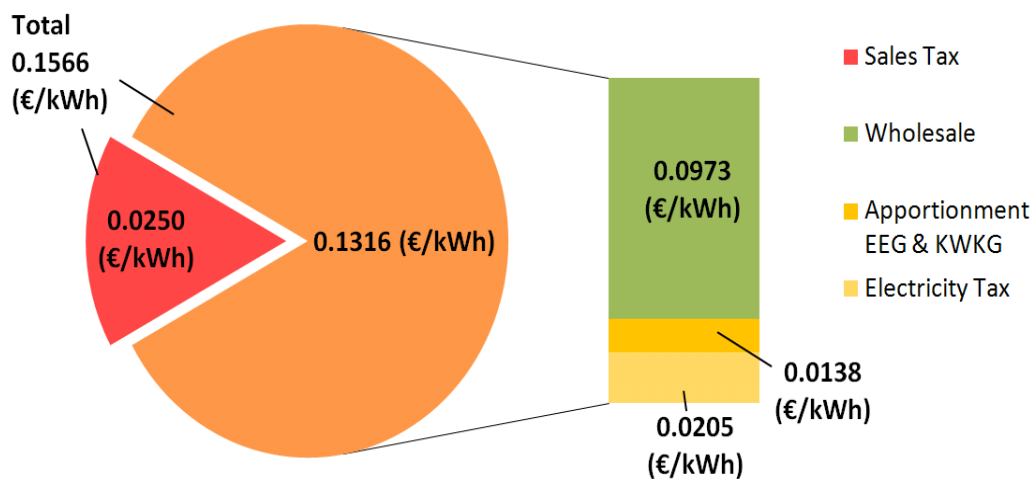
### 2) **Scenario 2: Demand rates as a measure for load management**

Scenario 2 is the extension of Scenario 1 in the sense that everything remains the same except for an additional demand rate that is charged for peak consumption each month. This scenario follows the logic of utility regulated prices as in the test case for the San Francisco office building (Momber et al. 2010), but in contrast to the implementation there, this charge is constant for all months and does not discriminate between the seasons. It is set at  $3 \text{ €/kW}$  peak consumption. The yearly demand rate remains in place.

### 3) Scenario 3: Historical, variable EEX prices 2009

To find the optimal operation schedule for the intermittent storage, the EMS of the Fraunhofer office building has access to prices pegged to the wholesale day-ahead market of the Physical Electricity Index (PHELIX base) at the EEX in Leipzig. The hourly varying prices for 2009 were downloaded from the official website (EEX 2009). As with the other input series, the set of 8760 data points was taken and aggregated to type days for each month. To fit the input demands of DER-CAM, negative prices were set to 0<sup>2</sup>. In a simplifying approach, the wholesale prices were then translated into end-user prices by adding static values for net access fees, concession levies, and payments from EEG and KWKG, as well as 19 % sales tax. Figure 6 shows the fixed proportions that are derived from today's flat rate tariff, i.e. the 2009 electricity bills which are assumed to be constant for the entire year.

Figure 6: Composition of end-user electricity prices



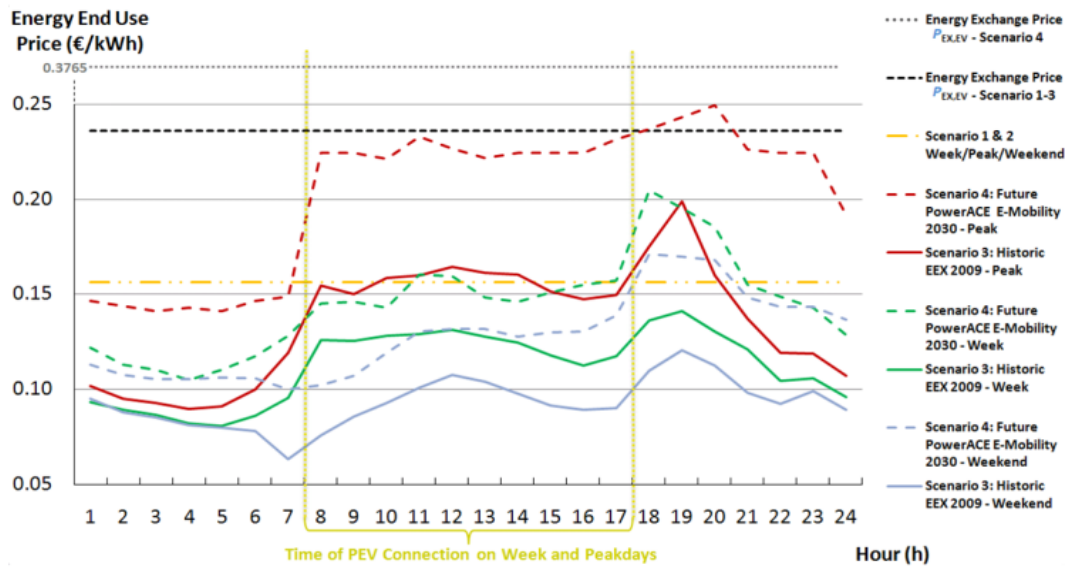
### 4) Scenario 4: Climate and E-Mobility – future variable EEX prices 2030

To develop future electricity price conditions, the modeling software PowerACE, an agent-based simulation was used, which was developed to assess the impacts of energy and emissions trading under increased renewable fluctuating energy generation (Sensfuß 2007). Spot prices for electricity are modeled using

<sup>2</sup> The changes are assumed to be insignificant as only three hourly instances of the weekend class are of concern throughout the whole year of analysis: October at 2 h and in December at 7 h and 8 h.

a marginal cost approach. Wholesale spot tariffs were translated into end-user prices by adding static values for net access fees, concession levies, and payments from the German feed-in law, as well as 19 % sales tax. The generation mix for 2030 is based on our own assumptions related to calculations in (Möst, Rosen, and Rentz 2007) and primary energy prices given in (International Energy Agency 2009). The penetration of renewable energies in 2030 is in the range of 60 % and taken from (Nitsch 2008). The marginal costs of intermittent renewable generation are assumed to be 0 euro per MWh. Therefore, high renewable generation results in lower spot prices. System assumptions concerning the load of grid-connected vehicles are in line with a scenario favorable to new technology with approximately 12 million PEVs and a demand of 17 TWh. “Charging after last trip” is used as the charging profile.

Figure 7 shows a summary of the above described price scenarios for the example month of January. The orange dot-and-dashed line indicates the flat prices,  $P_{supply} = 15.66 \text{ €ct/kWh}$ , for Scenarios 1 and 2 on all type days. The other six price curves represent the historical prices for 2009, Scenario 3 is shown as continuous lines, and Scenario 4, the future price scenario for 2030, is represented by dotted lines. Each the curves for the three type day classes: weekends in blue, weekdays in green and peak days in red. All the curves show peak price spikes in the early evening hours of 18 h – 20 h as well as low nighttime prices. All the 2030 prices are consistently higher than the 2009 ones and additionally show a higher price spread between the minimum and maximum price of the diurnal schedule: The type day weighted average of the hourly price for 2009 EEX (DER-CAM input) amounts to  $8.71 \text{ €ct/kWh}$ , and to  $13.90 \text{ €ct/kWh}$  in the 2030 PowerACE simulation of the EEX. It is important to note that the vehicles can be unfavorably connected in the sense that the highest differences in diurnal minimum and maximum hourly price can occur before or after the time of PEV connection marked by the curly bracket in yellow. It is not apparent for the selected month of January in this example illustration, but for other months it is possible that the peak price for Scenario 4 can be above the energy exchange price (e.g. in 11 h of June, July and October as well as 12 h of July and 17 h of November). For Scenarios 1 – 3,  $P_{EX,EV} = 23.6 \text{ €ct/kWh}$  remains constant, but the average residential price increases as well in 2030 in the future scenario 4. The upsurge is the same as the pro rata change in weighted average hourly price between 2009 and 2030, which is 59.53 % in total or a continuous 2.26 % p.a. Therefore the future energy exchange price amounts to  $P_{EX,EV,2030} = 37.8 \text{ €ct/kWh}$ .

Figure 7: Price curves for January by type days in Scenarios 1 – 4<sup>3</sup>

## 5 Results

A reference case was created for each of the price scenarios. Unlike the no-investment baseline case, the reference case depicts an optimization outcome for comparison, where all other technologies are forced into the solution set, but no PEVs are allowed. Comparing the two goal function values (with and without PEVs) directly with each other makes it possible to value the connection of the intermittent storage to the system.

The results on a yearly basis are summarized in Table 4, which shows the microgrid's savings and the corresponding cost components caused by PEV connection to the office building. In all scenarios of the business model application, cars are charged because the energy is valuable to the system, while the price spread between the energy exchange and the hourly electricity rate ( $P_{EX,EV} - P_{Supply}$ ) is the main driver of this behavior. However, the created value is fairly, i.e. evenly, distributed among the participants. The microgrid always pays a connection payment to redistribute the gain and create a win-win situation for both the PEV owners and the energy system. The benefit sharing values for connection payments ( $V$ ) are indicated in the blue cells. The total and percentage cost savings generated are marked in the green cells. These "profits" are

<sup>3</sup> These prices are merely an example and depict the month of January.

net, i.e. all costs are already taken into account, including the compensation for battery usage and degradation, marked by the red cells. Furthermore, the cash flow arising from the net energy exchange has the sign in the direction of PEVs paying the building for battery charges. To give an example, in Scenario 3, the microgrid functions without PEVs and has a yearly energy bill of €65,439. Connecting PEVs is incentivized by paying an annual contribution of 2.667 €/kWh to the owners of the vehicles, which the EMS handles like an investment in price response capability. The batteries are operated under the building's control and the owners of the PEVs are compensated for the accruing battery degradation with €1,110. Having paid for the connection and battery wear, the microgrid's resulting cost savings amount to €2,310 or 3.53 % of the reference case cost. The connection payments and the cost savings can both be understood as indicators for the value of the batteries to the system. Obviously, the more the storage contributes to cost savings, the more benefit can be shared via (V). In all cases, battery degradation is significant and can be understood both as an indicator for battery usage (directly proportional to energy processed) and a main determinant of battery economics. In the example of Scenario 1, for instance, the created value before sharing would have been €3075 without degradation costs instead of €2076, i.e. 48.8 % higher than with degradation costs.

In summary, it can be observed that the scenarios with variable prices tend to assign higher value to the storage than scenarios with regulated tariffs. Scenario 2 has the lowest gain in percentage of the reference cost, because the demand charge counteracts the value creating charge of the vehicles.



Table 4: High Level Numerical Summary - ISI Cost Minimization

Price scenarios <sup>4</sup>	1 ISI today	2 Demand charge	3 EEX 2009	4 Power-ACE 2030
Reference case cost	81,716	84,518	65,439	79,366
Benefit sharing connection payment ( $V$ ) = [€/kWh]	1.1982	1.0141	2.6670	4.7541
Compensation for battery degradation [€]	1,099	1,019	1,110	1,458
Mutual cost savings [€]	1,038	878	2,310	4,117
In % of the total bill	1.27%	1.04%	3.53%	5.19%
Operation schedule	Figure 9	Figure 10 - Figure 13	Figure 14 - Figure 15	Figure 16 - Figure 17

Comparing Scenarios 3 and 4, one has to acknowledge that the higher price volatility during the time of PEV connection, as well as the increased price spread ( $P_{EX,EV} - P_{Supply}$ ) create higher battery usage and therefore more value. In the following, PEV operating schedules and microgrid interactions are discussed in more detail for each scenario.

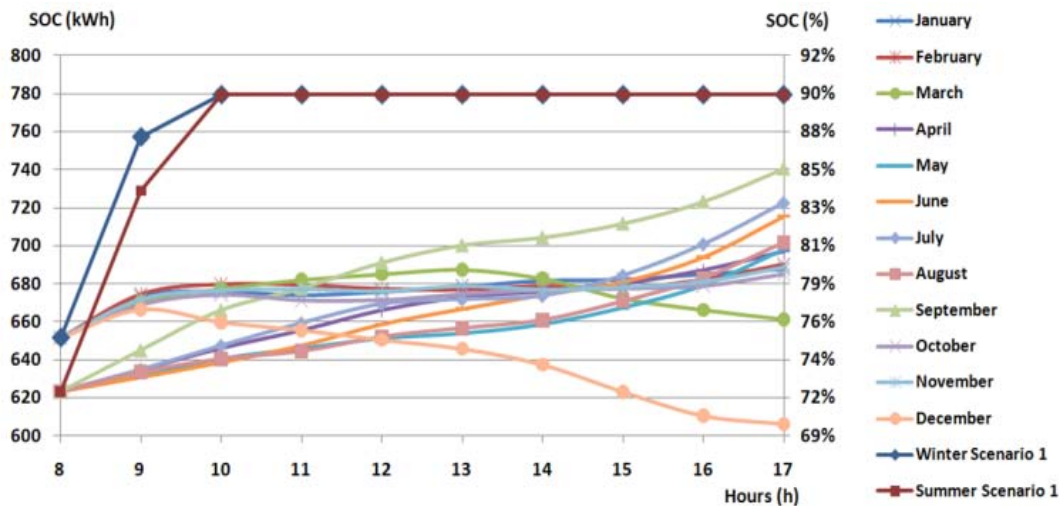
It is worth taking a closer look at the PEV operation schedules for Scenarios 1 and 2. To analyze the impact of the tariff difference, the SOC of the connected PEVs is evaluated over time. Figure 8 shows the effect of the demand charge on the ISI tariff. In Scenario 1, the two upper curves, the SOC rises immediately after connection and never changes value, in fact there is charging every hour to counteract the decay losses of maintaining the charge. However, for Scenario 2 (all other curves), the SOC adapts to the dictation of economic conditions in a different way. In interaction with the CHP units, the batteries are used for peak shaving and load leveling. In winter, the  $SOC_{out}$  is slightly lower than in summer<sup>5</sup>. This is based on the free CHP (sprint) capacity in summer, most of which can be used for peak shaving as excess heat can dissipate at no cost,

<sup>4</sup> All scenarios were tested with an aggregated battery storage of 866 kWh.

<sup>5</sup> Even though the demand charge is constant over the year. March and December show this behaviour in its extremes.

while in winter the entire volume is occupied by monetary savings from heat generation. For the CHP system, it is thus more economic to create efficiency gains than lower the resulting utility electricity consumption to avoid demand charges.

Figure 8: PEV Operation schedules on peak days for Scenarios 1 and 2



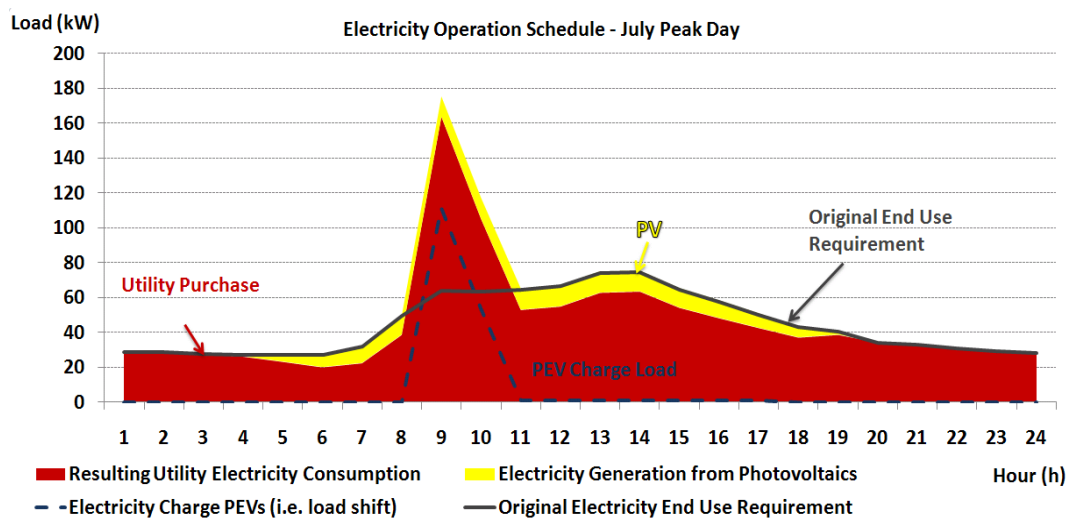
### A. Results price Scenario 1 – ISI tariff today

The composition of the energy generation needed to meet the original end-use requirement (continuous dark gray line) of a January weekend and a peak day in Scenario 1 is shown in Figure 9. The yellow area denotes the electricity generated from the PV system during the day. The dark red area represents the purchases from the supply network by the utility company, which equal the residual load not met by other generators (in July only the PV system), except for additional battery charges and discharges.

The resulting PEV load is called “dumb” charging because the tariff creates no incentive to use the storage or load shifting on any type day (week or peak). On the contrary, the price spread between the industry  $P_{Supply}$  and the residential tariff  $P_{EX,EV}$  actually creates an incentive for the cost-optimizing microgrid to charge the PEVs as much and as quickly as possible, shown by the dashed blue line. This creates a situation where the additional load for charging the PEVs is, in terms of the system load to the supply network, least favorably met. The spikes in the residual load curve are cost irrelevant to the program because the tariff lacks incentives to reduce peak demand. The significant *yearly* demand rate of €8226 (10.2 % of the total bill) may contribute to shaving one or

two peak months of the year but is deficient overall. The new peaks from connecting PEVs at 9 h amount to approximately 160 kW, more than twice the original crest (74.6 kW on peak days and 62.8 kW on weekdays) of the end-use requirement. The microgrid optimizes its own operation but not in a way which is desirable for the supply network and the energy system as a whole. The peaks are unmotivated and unintelligently scheduled.

Figure 9: Diurnal Microgrid Analysis for Peak Days in Scenario 1<sup>6</sup>

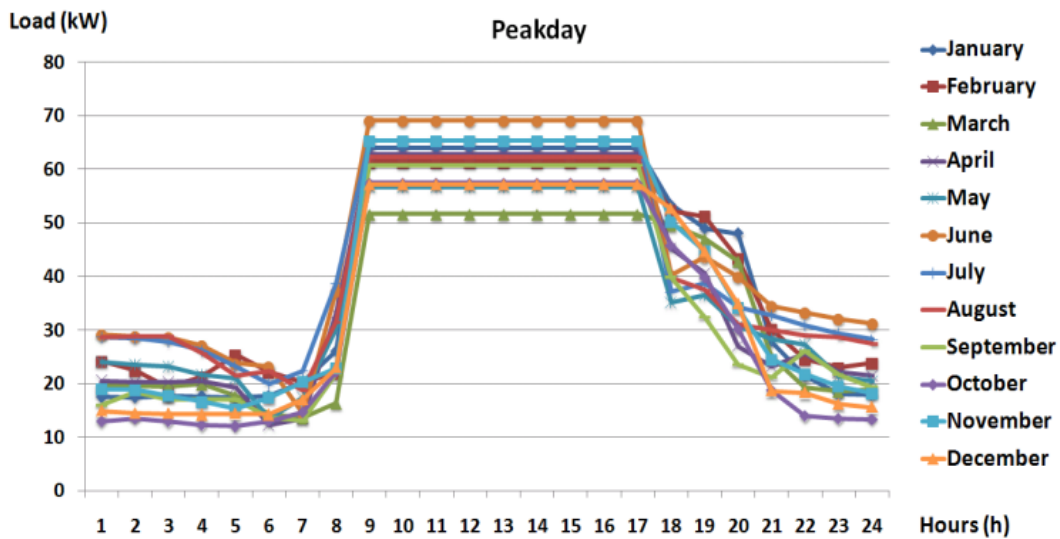


## B. Results price Scenario 2 – ISI tariff with monthly demand charge

In this scenario, cars are still charged but the *monthly* demand charge of 3 €/kW peak consumption proves to be a powerful measure and an effective policy for reducing peak electricity consumption. Figure 10 shows the resulting utility electricity purchases in kW for peak days of all months. As we saw in the test case, all curves are capped at certain levels and loads are rigorously shifted.

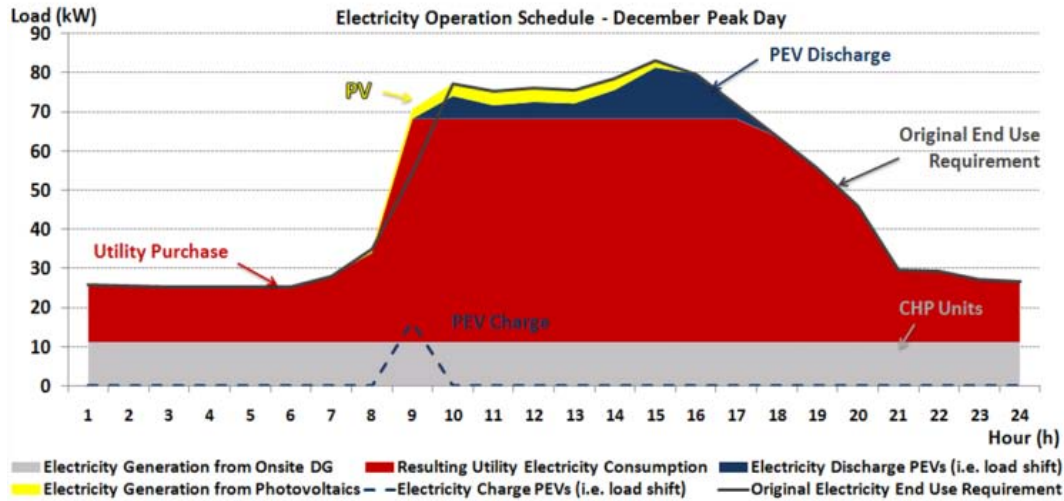
<sup>6</sup> The operating schedule for weekdays is very similar.

Figure 10: Resulting utility electricity purchases on peak days: Scenario 2



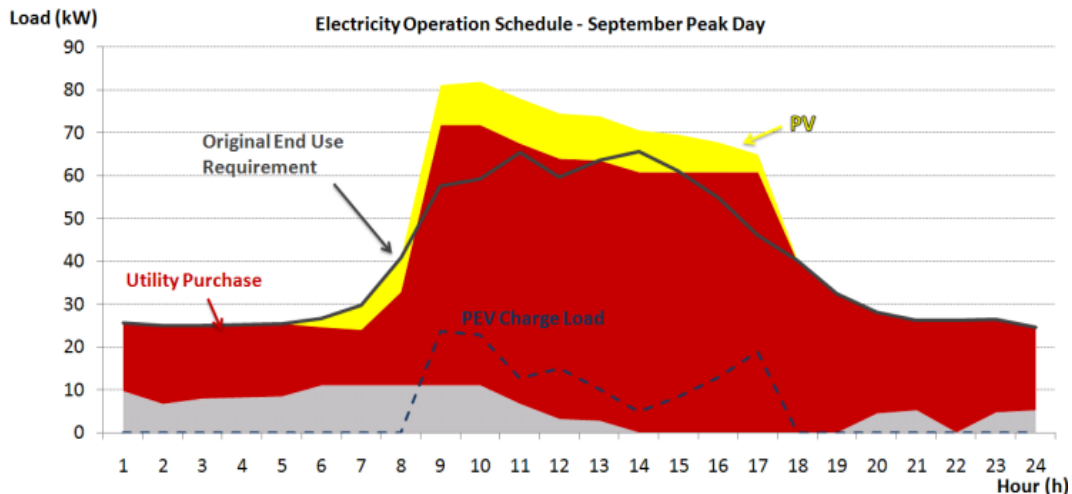
It is now interesting to examine how this peak shaving is done using the PEV batteries in competition with the other options. Since PV production is rigid (non-controllable) and directly proportional to the insolation weighted with the average efficiency (in this case set to 13 %), the only other degree of freedom is provided by the engaging and disengaging of the CHP units. The efficient and therefore economic operation of the CHP units, however, is dependent on heat coinciding with electricity demand. Figure 11 shows the electricity operation schedule of a peak day in December and, analogously, Figure 12 illustrates this correlation for September. In both diagrams the gray base band represents the electricity generation by CHP units and the dark blue area is the energy provided by the PEV storage system. Because the office building has a concurrent high heat demand in winter, the system utilizes the CHP unit to produce electricity at full power all day. Due to the high economic incentive to lower peak demand, the PEV batteries are now used to provide a share of the electricity. Although the price spread between the industry  $P_{Supply}$  and the residential tariff  $P_{EX,EV}$  would otherwise forbid this in fiscal terms, the batteries remain the only lever to lower the spikes between 10 h and 17 h. Note that batteries are discharged over the entire day while the  $SOC_{out}$  is still sufficiently high for travel purposes.

Figure 11: Electricity balance: microgrid analysis December peak day: Scenario 2



In September, on the other hand, a month in-between the seasonal extremes, a different operation of the system is apparently cost optimal. Instead of discharging the batteries, they now provide a sink for electricity. However, the charge is well timed, causing the net electricity consumption from the utility company to be completely flat (Figure 12).

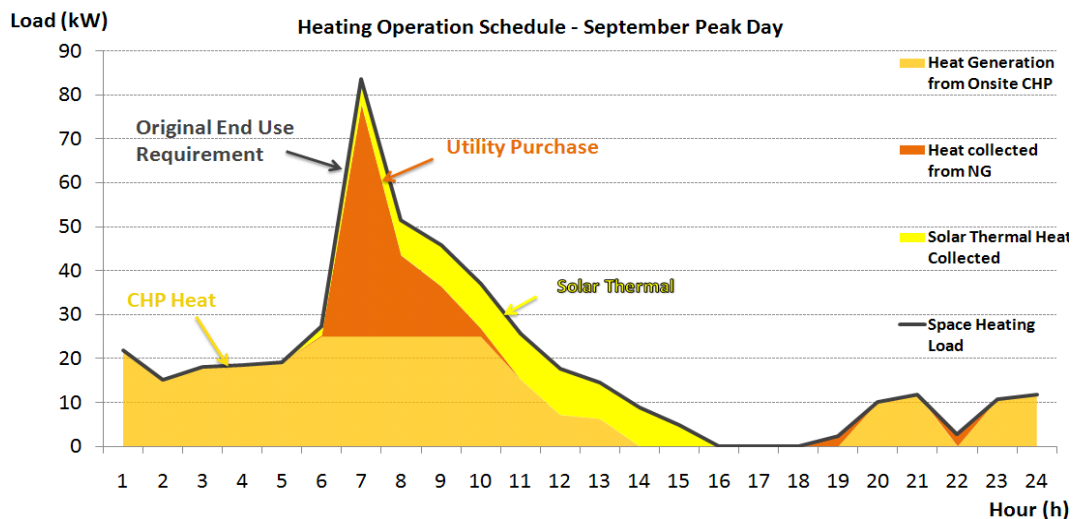
Figure 12: Electricity balance: microgrid analysis September peak day: Scenario 2



The heat balance depicted in Figure 13 provides insights into how volatile the end-use requirement is and which generation technologies are dispatched in

order to meet the demand. Here, the yellow-shaded area represents the heat collected from the solar thermal units, while the beige area shows the recovered waste heat from the CHP units. The remainder of the demand, shown in orange, is met by the gas fired heating boilers, i.e. grid purchases. It is interesting to see how the prevailing heat demand in the morning up to 13 h renders CHP operation economically profitable which affects the electricity balance. Shortly thereafter the profitable window for PEV battery discharge closes and the energy generated from PV and grid purchases is used to charge the battery for the drive home. Thus, during connection, the batteries jump in with intelligent charging to keep the peak shaved. Note that even though it seems utility purchases decrease between 9 h and 15 h (cf. Figure 12), without battery support, they could not have been kept constant at the load level of approximately 60.8 kW.

Figure 13: Heat balance: microgrid analysis September peak day: Scenario 2



### C. Results price scenario 3 – EEX 2009

In Scenario 3, the microgrid has access to variable end-user prices which are determined by the wholesale price of the EEX. The question arises here as to what impact these variable prices have on the integration of electric vehicles in the microgrid. In theory, the range of prices should make the use of storage more attractive. The program finds the optimal solution for its purchases depending on the prices during the day, utilizing the connected storage system to dispatch generators and loads if this is the most economic option. The results

show that PEV charging and discharging is used as an economic option to react to price signals from the energy market.

Figure 13 shows how the microgrid behaves given a varying electricity rate pegged to the EEX on a peak day in May 2009. The vertical, dashed blue lines indicate the time of PEV connection and the dashed red line marks the diurnal run or the electricity price in €/MWh shown on the right-hand vertical axis. The CHP engines run continuously during the day until 16 h when heat demand drops. At the same time, the hourly electricity price reaches its minimum and the variable share of electricity demand is scheduled to exploit this, i.e. the PEVs are charged between 16 h and 17 h before disconnecting.

Figure 14: Electricity balance: microgrid analysis May peak day: Scenario 3

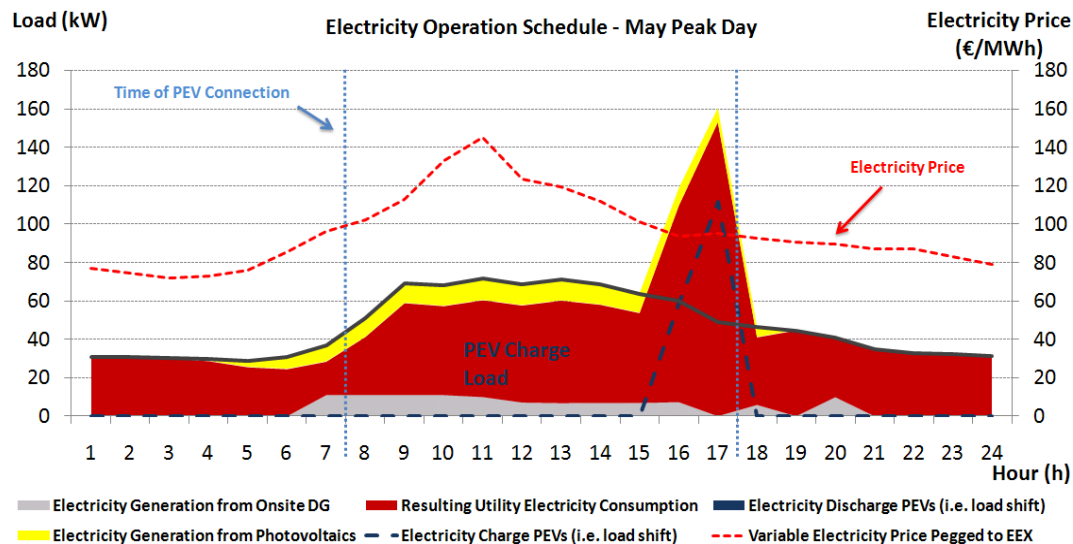
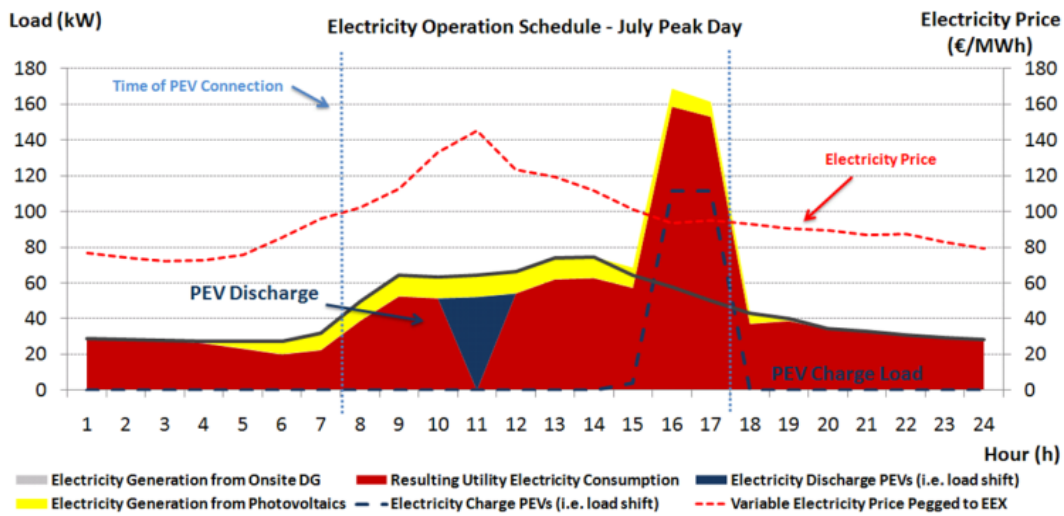


Figure 14 depicts the same electricity balance in conjunction with the hourly varying energy price for peak days of July 2009. In general, a similar reaction to the price signal can be observed. The price curves are almost identical, both with a maximum of 145.3 kW at 11 h. PEV charging is done during the two hours of minimum prices: 16 h and 17 h. However, there is no coincident heat demand in this summer month and therefore CHP units are not used. Consequently, PEV batteries are used for demand scheduling and avoiding peak prices via a significant discharge of 52.2 kW. At 11 h, the only generators available to meet the end-use electricity requirement are the PV system and the connected PEV batteries.

Figure 15: Electricity balance: microgrid analysis July peak day: Scenario 3



#### D. Results price scenario 4 – PowerACE 2030

In Scenario 4, variable end-user prices are pegged to the wholesale price of the EEX simulated by PowerACE for the year 2030. Having demonstrated that the program is capable of reacting to hourly varying prices, it seems interesting to analyze whether the storage in the future will become even more valuable to the microgrid and if so, for what reasons. Again, the theory leads us to predict that an increased price spread between high price hours and low price hours should make storage use comparatively more attractive.

The same general effects can be observed when comparing Scenarios 3 and 4 with each other. However the use of the storage system is even more extreme in Scenario 4. Figure 16 shows the operation of the microgrid including the connected PEV batteries in conjunction with the concomitant price curve for the peak day class in May. The highest prices are for 11 h and 12 h. In order to avoid purchasing power at these times, the batteries are completely discharged and are able to fully substitute utility purchases of 50.3 kW and 50.4 kW. After an idle hour at 13 h, batteries are then continuously charged for the next three hours with the cost of 151.5 €/MWh, 158.2 €/MWh and 157.1 €/MWh. Another interesting effect can be seen when comparing the electricity balances in May for Scenarios 3 and 4 with each other. The higher electricity prices in Scenario 4 make onsite generation by the CHP units more valuable to the microgrid. Whereas in Scenario 3 the DG units were only operated between 7 h and 20 h, in Scenario 4 they run for 24 hours.



Figure 16: Electricity balance: microgrid analysis May peak day: Scenario 4

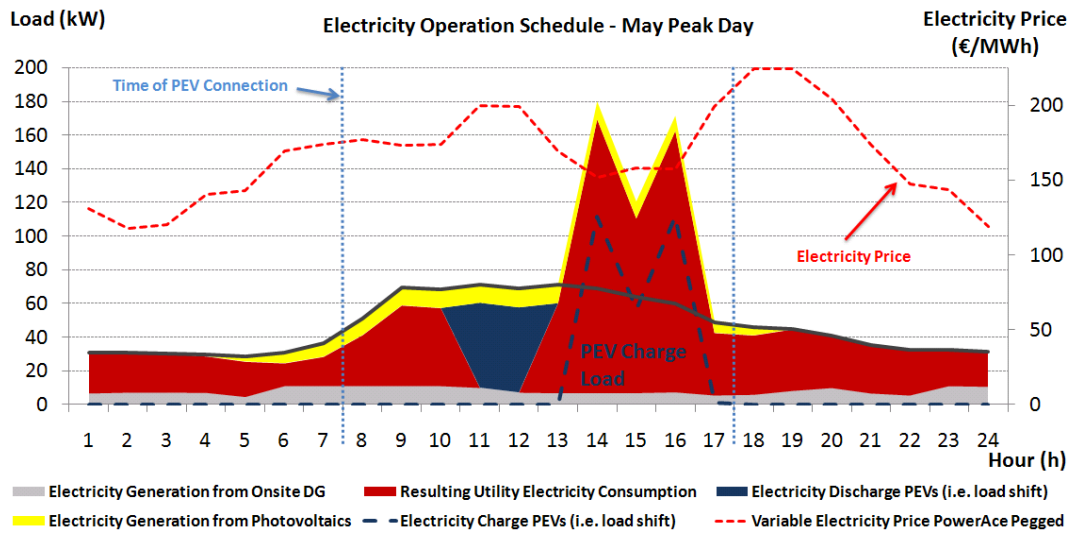
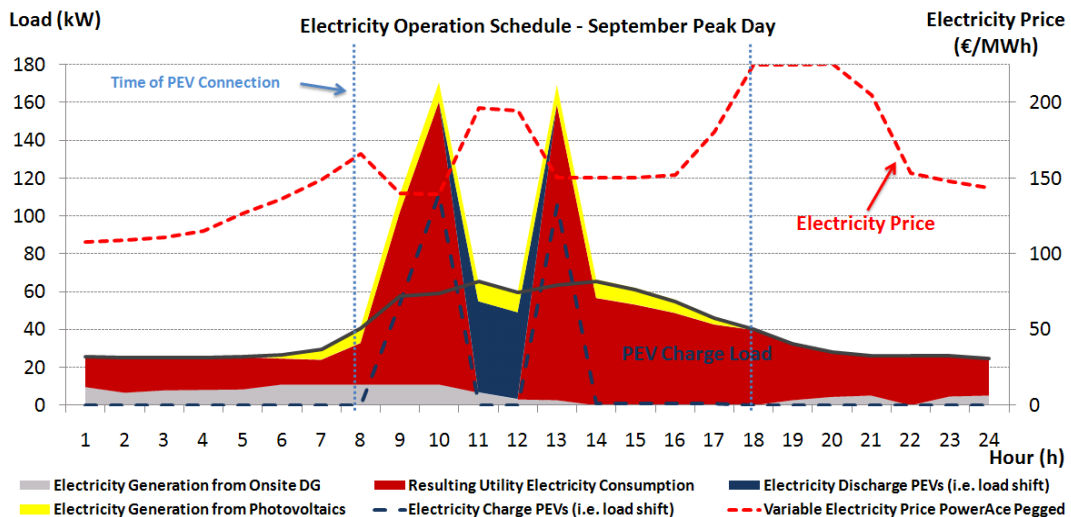


Figure 16 provides another example of intense peak shifting according to price dictation. In the microgrid analysis for the September peak day, it is apparent that the first load peak created from charging PEVs arises at 5 h and 10 h when the electricity prices are the lowest (140.2 €/MWh and 139.5 €/MWh) during PEV connection. The electricity price then rises to its maximum during PEV connection for the next two hours and hence the batteries are used to provide energy of 48.2 kW and 45.9 kW, respectively.

Figure 17: Electricity balance: microgrid analysis September peak day: Scenario 4



## 6 Conclusion

This paper has shown that connecting plug-in electric vehicles to the microgrids in office buildings can be profitable under the proposed business contract conditions. However, even under idealized conditions with optimistic assumptions, the value for the building's energy management system is relatively low. In addition, the study quantified this value and defined determinants for it when introducing an appropriate scheme. The different pricing schemes and their effects on the operation of intermittent storage have been revealed and examined in detail.

### A. Summary and comparison of results from Scenarios 1 – 4

The connected fleet of PEVs with an aggregated storage of 866 kWh is significant in its size<sup>7</sup>. Thus the potential impact of connecting such a storage array is high and requires intelligent scheduling. In Scenario 1, it was shown that the “dumb charging” schedule arising from today's tariff is not suitable for integrating PEVs into the EMS of office buildings. This causes undesired demand spikes which are inconvenient for any operation planning. In Scenario 2 with demand charges, it was shown that there is a favorable interaction of PEVs and microgrids, and with CHP systems in particular, as peak loads are decreased and shifted to other times. The results of Scenario 3 and 4 showed that variable prices lead to a *desired* microgrid reaction to market signals. The consumption peaks are *desired* because prices indicate that generation resources are abundant and should be used at those times to benefit the system. However, it has to be noted that the utilization of the local transformer is not considered. In fact, this study assumed the absence of load flow grid constraints such as thermal line limits and optimal voltage zones.

This study evaluated two fundamentally different pricing schemes for the same end-use requirements. The demand charge is very effective for load leveling, but lacks the flexibility to react to unplanned exogenous price signals. Under the assumption that a flat load curve is always optimal, this policy should be chosen. The system is predictable but inflexible. The other paradigm, reactivity to variable prices, can be perceived as an effective way to elicit demand-side responses. In essence, this system is about load shifting as well, but it does not

---

<sup>7</sup> For comparison: the weighted average daily consumption over all week- and peak days is 1020 kWh. This does not include weekend days but does consider hours 1 through 24, i.e. also those when the PEVs are not connected.

create load leveling. The inherent assumption behind this approach is that the price differences stem from a market that accurately mirrors the supply and demand for energy. Therefore, the spikes caused are desirable for the system and have to be evaluated differently to unmotivated peak demands. In this analysis variable prices which influence the charging load and operation schedule of the PEVs have been shown to be a good lever to increase system stability. This supports the thesis that markets are an efficient tool to operate energy systems and allocate generation capacity.

## **B. Model extension**

The Distributed Energy Resources Customer Adoption Model, a mixed integer linear optimization program that minimizes the yearly energy costs for a microgrid, was modified in this study. The model was conceptually extended and implemented in the General Algebraic Modeling System to account for plug-in electric vehicles. A degradation model was adapted to economically value the wear-out of batteries due to cycling. Altogether, the inaugurated model extensions can serve as a basis for future scientific research in new sub disciplines and the field of grid applications, such as vehicle-to-grid or battery-to-grid interactions.

Based on the common understanding that plug-in electric vehicles along with distributed generation can create economic and environmental benefits for societies, a case study was presented which juxtaposes the current situation in Germany with simulated future scenarios focusing on the economic impact of plug-in electric vehicle connection to a microgrid with on-site generation units.

Analyzing this German case showed that the lower marginal costs for pooling connection at the grid access points of office buildings are favorable if intelligent energy management systems are in place. Connecting an entire fleet of commuter vehicles to an optimized microgrid environment also implies certain economies of scale. Coincident with peak heat and electricity loads as well as solar radiation, the plug-in electric vehicle connection allows for shifting energy demand as desired for cost savings.

## 7 Acknowledgements

This work was supported by the Office of Electricity Delivery and Energy Reliability's Smart Grids Program in the U.S. Department of Energy under Contract No. DE-AC02-05CH11231.

This paper was written based on the master thesis document by Sebastian Beer and Ilan Momber, who both spent a research visit at the Lawrence Berkeley National Laboratory (LBNL). The optimization tool used within this work, the Distributed Energy Resources - Customer Adoption Model (DER-CAM), has been designed by Lawrence Berkeley National Laboratory, California for several years. The authors of this paper would like to express special thanks to all members of the DER-CAM development team at LBNL for their support, in particular Michael Stadler, Chris Marnay, Judy Lai, and Afzal Siddiqui.

The application of the model to a German use case has been co-financed under a grant of the German Federal Ministry of Education and Research (BMBF) as part of the project "Fraunhofer Systems Research Electric Mobility" under project number 13N10599. We thank Gillian Bowman-Köhler for discussions and critical reading of the manuscript.

## 8 References

Axsen, Jonn, Andrew Burke, and Kenneth S Kurani. 2008. *Batteries for Plug-in Hybrid Electric Vehicles ( PHEVs ): Goals and the State of Technology circa 2008. Technology*. Davis, CA.

[http://pubs.its.ucdavis.edu/download\\_pdf.php?id=1169](http://pubs.its.ucdavis.edu/download_pdf.php?id=1169).

Beyer, Catharina, Christoph Heinemann, and Tobias Tusch. 2009. *Einführung von lastvariablen und zeitvariablen Tarifen*.

<http://www.bundesnetzagentur.de/cae/servlet/contentblob/153298/publicationFile/6483/EcofysLastvariableZeitvariableTarife19042010pdf.pdf>.

Dürr, Dietmar. 2010. Quo Vadis Strompreise. *Energiewirtschaftliche Tagesfragen*, no. 60: 54-58.

EEX. 2009. European Energy Exchange: Market Data Download.

<http://www.eex.com/en/Download>.

- EnWG. 2005. *Gesetz über die Elektrizitäts- und Gasversorgung (Energiewirtschaftsgesetz - EnWG)*.  
[http://bundesrecht.juris.de/bundesrecht/enwg\\_2005/gesamt.pdf](http://bundesrecht.juris.de/bundesrecht/enwg_2005/gesamt.pdf).
- EURELECTRIC. 2010. Market Models for the Roll-Out of Electric Vehicle Public Charging Infrastructure. *EURELECTRIC Concept Paper*.
- GAMS Development Corporation. 2009. GAMS® Solver Description in the on-line documentation. <http://www.gams.com/docs/document.htm>.
- IBM ILOG. 2009. GAMS/CPLEX Solver Manual.  
<http://www.gams.com/dd/docs/solvers/cplex.pdf>.
- International Energy Agency. 2009. *World Energy Outlook 2009*. OECD/IEA.  
<http://www.worldenergyoutlook.org/2009.asp>.
- KEMA Inc. and ISO/RTO Council. 2010. Assessment of Plug-in Electric Vehicle Integration with ISO / RTO Systems, no. March.
- Kempton, Willet, and Jasna Tomic. 2005. Vehicle-to-grid power fundamentals: Calculating capacity and net revenue. *Journal of Power Sources* 144, no. 1 (June): 268-279. doi:10.1016/j.jpowsour.2004.12.025.  
<http://linkinghub.elsevier.com/retrieve/pii/S0378775305000352>.
- Lopes, João A. Peças, Filipe Joel Soares, and Pedro M. Rocha Almeida. 2011. Integration of Electric Vehicles in the Electric Power System. *Proceedings of the IEEE* 99, no. 1 (January): 168-183.  
doi:10.1109/JPROC.2010.2066250.  
<http://ieeexplore.ieee.org/lpdocs/epic03/wrapper.htm?arnumber=5593864>.
- Marnay, C., G. Venkataramanan, M. Stadler, a.S. Siddiqui, R. Firestone, and B. Chandran. 2008. Optimal Technology Selection and Operation of Commercial-Building Microgrids. *IEEE Transactions on Power Systems* 23, no. 3 (August): 975-982. doi:10.1109/TPWRS.2008.922654.  
<http://ieeexplore.ieee.org/lpdocs/epic03/wrapper.htm?arnumber=4519391>.
- Momber, Ilan, Tomás Gómez San Román, Michel Rivier, and Rafael Cossent. 2011. *Merge D5.1 - New Actors and Business Models for the Integration of Electric Vehicles*. [http://www.ev-merge.eu/images/stories/uploads/MERGE\\_WP5\\_D5.1.pdf](http://www.ev-merge.eu/images/stories/uploads/MERGE_WP5_D5.1.pdf).

- Momber, Ilan, Tomás Gómez, Giri Venkataramanan, Michael Stadler, Sebastian Beer, Judy Lai, Chris Marnay, and Vincent Battaglia. 2010. Plug-in Electric Vehicle Interactions with a Small Office Building : An Economic Analysis using DER-CAM. In *IEEE Power and Energy Society General Meeting*. Minneapolis. <http://der.lbl.gov/publications/plug-electric-vehicle-interactions-small-office-building-economic-analysis-using-der-cam>.
- Möst, D., J. Rosen, and O. Rentz. 2007. Renewable electricity generation until 2020 in Europe - A model based approach. In *Proceedings of the Internationale Energiewirtschaftstagung*. Vienna: IEWT.
- Nitsch, Joachim. 2008. *Leitstudie 2008: Ausbaustrategie Erneuerbare Energien, Aktualisierung und Neubewertung bis zu den Jahren 2020 und 2030 mit Ausblick bis 2050*. [http://www.bmu.de/erneuerbare\\_energien/downloads/doc/42383.php](http://www.bmu.de/erneuerbare_energien/downloads/doc/42383.php).
- Pesaran, Ahmad, Kandler Smith, and Tony Markel. 2009. Impact of the 3Cs of Batteries on PHEV Value Proposition: Cost, Calendar Life, and Cycle Life (Presentation). In *Renewable Energy*.
- Peterson, Scott B., Jay Apt, and J.F. Whitacre. 2010. Lithium-ion battery cell degradation resulting from realistic vehicle and vehicle-to-grid utilization. *Journal of Power Sources* 195, no. 8 (April): 2385-2392. doi:10.1016/j.jpowsour.2009.10.010. <http://linkinghub.elsevier.com/retrieve/pii/S0378775309017443>.
- Peterson, Scott B., J.F. Whitacre, and Jay Apt. 2010. The economics of using plug-in hybrid electric vehicle battery packs for grid storage. *Journal of Power Sources* 195, no. 8 (April): 2377-2384. doi:10.1016/j.jpowsour.2009.09.070. <http://linkinghub.elsevier.com/retrieve/pii/S0378775309017303>.
- Photovoltaic Geographical Information System (PVGIS). 2009. The European Commission Tool for Geographical Assessment of Solar Resource and Performance of Photovoltaic Technology. <http://re.jrc.ec.europa.eu/pvgis/>.
- Rutschmann, Ines, and Jochen Siemer. 2009. Price Development Analysis of Photovoltaic Solar Power Plants. *Photon* 09.
- Sensfuß, Frank. 2007. Assessment of the impact of renewable electricity generation on the German electricity sector An agent-based simulation approach.

SIDDIQUI Afzal S., Chris MARNAY, Jennifer L. EDWARDS, Ryan M. FIRESTONE, Srijay GHOSH, and Michael STADLER: *“Effects of a CarbonTax on Microgrid Combined Heat and Power Adoption,”* Journal of Energy Engineering, American Society of Civil Engineers (ASCE), SPECIAL ISSUE: QUANTITATIVE MODELS FOR ENERGY SYSTEMS, April 2005, Volume 131, Number 1, page 2 – 25, ISSN 0733-9402.

STADLER Michael, Chris MARNAY, Ratnesh SHARMA, Gonçalo MENDES, Maximillian KLOESS, Gonçalo CARDOSO, Oliver MÉGEL, Afzal SIDDIQUI: *“Modeling Electric Vehicle Benefits Connected to Smart Grids,”* 7th IEEE Vehicle Power and Propulsion Conference, Sept 6-9 2011, Chicago, IL 60604, USA, LBNL-4929E.

Verbund Kommunalen Unternehmen. 2006. Analyse des nationalen Potenzials für den Einsatz hocheffizienter KWK und hocheffizienter Kleinst-KWK.  
[http://www.vku.de/de/Energiewirtschaft/Handel\\_Vetr.\\_Erzeugung/KWK/KWK\\_-\\_Hintergrundinfos/10.07.06\\_15\\_kwk\\_17.pdf](http://www.vku.de/de/Energiewirtschaft/Handel_Vetr._Erzeugung/KWK/KWK_-_Hintergrundinfos/10.07.06_15_kwk_17.pdf).



Authors' affiliations:

David Dallinger  
Martin Wietschel

Fraunhofer Institute for Systems and Innovation Research (Fraunhofer ISI)  
Competence Center Energy Policy and Energy Systems

Ilan Momber  
Tomás Gomez

Instituto de Investigación Tecnológica (IIT) Madrid, Spain

Sebastian Beer  
RWE Innogy GmbH, Hamburg, Germany

Contact: Brigitte Kallfass  
Fraunhofer Institute for Systems  
and Innovation Research (Fraunhofer ISI)  
Breslauer Strasse 48  
76139 Karlsruhe  
Germany  
Phone: +49 / 721 / 6809-150  
Fax: +49 / 721 / 6809-203  
E-mail: [brigitte.kallfass@isi.fraunhofer.de](mailto:brigitte.kallfass@isi.fraunhofer.de)  
URL: [www.isi.fraunhofer.de](http://www.isi.fraunhofer.de)

Karlsruhe 2011